

Theory of muon spin relaxation of gaseous C_2H_4Mu

Ralph Eric Turner

Department of Physics, Northwest Community College, 5331 McConnell Avenue, Terrace, British Columbia, Canada V8G 4C2

R. F. Snider

Department of Chemistry, University of British Columbia, Vancouver, Canada V6T 1Z1

(Received 11 July 1996)

A theoretical study of the muon spin relaxation of the gaseous muonated ethyl radical C_2H_4Mu is expanded in this paper to include both longitudinal and transverse signals. This study is based upon an operator expansion of the spin-density operator for the radical with its time dependence described by the linearized quantum Boltzmann equation. Relaxation is due to collisions which reorient the radical's rotational angular momentum while effects on the muon's spin are due to couplings between the muon's spin, the radical's free-electron spin, and the radical's rotational angular momentum. The coefficients of the radical's spin Hamiltonian and the collisional lifetimes (cross sections) are used as fitting parameters to describe the transverse signals. A fit to the transverse data by itself and a global fit to both the transverse and longitudinal data are obtained with good accuracy. [S1050-2947(96)02812-0]

PACS number(s): 36.10.-k, 51.60.+a

I. INTRODUCTION

Experiments on the muon spin relaxation (μ SR) of the muonated ethyl radical C_2H_4Mu have been performed in longitudinal and transverse configurations [1-4]. A phenomenological equation [1-4] has been developed to describe the T_1 and T_2 relaxation times associated with these experiments while a theoretical [5] approach to the T_1 relaxation time has been developed. It is the purpose of this paper to reexamine the fit to the longitudinal data and extend the theoretical study to the transverse experiments. The phenomenological approach and the current theoretical approach are equally successful in fitting the pressure and field dependence of the transverse signals. Indeed, the fits produce essentially the same plots for the pressure and field dependence of the transverse signal. As well, both the phenomenological approach and the theoretical approach are successful in fitting all the pressure and field dependences of both the transverse and longitudinal signals with single sets of parameters. Both fits are about equally good.

In μ SR experiments [6,7], the dynamics of an ensemble of muon spins are followed through observation of the decay positrons which are emitted preferentially along the muon spin direction. Histograms of these ensembles are fitted to a count function,

$$N(t) = N_0 e^{-t/\tau_\mu} [1 + S(t)] + B_0, \quad (1)$$

where $\tau_\mu = 2.2 \mu\text{sec}$ is the lifetime of the muon, N_0 is a normalization constant, B_0 is a background constant, and $S(t)$ is the observed signal. These experiments are usually performed in one of two configurations, namely, a longitudinal setup where the incoming muon's spin and the magnetic-field direction are collinear and a transverse setup where they are perpendicular. The observed signals $S(t)$ may be theoretically described by the ensemble averaged behavior of a single muon's spin time dependence. For the ethyl radical experiments [1-4], the assumed forms of these signals are

$$S_L(t) = e^{-\lambda_L t} A_L \quad (2)$$

for the longitudinal configuration and

$$S_T(t) = e^{-\lambda_T t} \cos(\omega_T t + \theta_T) A_T \quad (3)$$

for the transverse configuration. The relaxation rates are then interpreted in terms of the relaxation times as follows:

$$\lambda_L = \frac{1}{T_1},$$

$$\lambda_T = \frac{1}{T_2} + \lambda_{T0}, \quad (4)$$

where λ_{T0} is inversely proportional to the total pressure P ,

$$\lambda_{T0} = \frac{\eta_0}{P}, \quad (5)$$

with η_0 an experimental fitting constant. λ_{T0} contributes to the overall relaxation rate due to field inhomogeneity over the stopping distribution of the muon in the gas [1-4]. In transverse fields the oscillatory time dependence associated with an observed frequency ensures that the signal being observed is due to a single relaxation mode. However, in longitudinal fields, this is not necessarily the case as more than one zero-frequency mode might be contributing to the observed signal. It is then a matter of fitting the signal to a sum of exponentials with differing amplitudes. For the theoretical description adopted in Ref. [5], the longitudinal signal was assumed to be a single exponential determined by the slowest relaxation rate. In the present extension of this study the amplitudes of the various relaxation modes are calculated as well as the relaxation rates and only those modes with appreciable amplitudes are considered. From a fitting point of view, the transverse field results are the more easily inter-

preted since they have a definite frequency and this aids in the selection of which single mode is being observed.

In attempting a theoretical study of the spin dynamics of the muonated ethyl radical a number of assumptions are needed. These assumptions fall into three broad categories of dynamical behavior, namely, the roles of thermalization, spin dynamics, and collision dynamics.

In the first category and under the present approach [5], it is assumed that the muon thermalizes in the muonated radical so that the initial state of the system is $C_2H_4\mu$ with only the muon spin initially polarized, i.e., having a preferred laboratory direction. That is, since no thermal muonium is detected in the transverse field experiment, it is assumed that muonium forms epithermally and reacts with the ethylene before thermalization is complete. This assumption ignores the possibility of the formation of thermal muonium with a very rapid reaction to form the radical. These are considered to be reasonable assumptions.

The next set of assumptions deal with the free evolution of the radical and its angular momentum properties. This radical has an electron spin \mathbf{S} , a muon spin \mathbf{I} , and four hydrogen spins \mathbf{I}_H , as well as a rotational angular momentum \mathbf{J} , and various vibrational, bending, and torsional modes. To include all of these dynamical quantities, which are all expected to be coupled, would lead to an extremely large basis set and also to the question of whether the experimental data are either accurate enough, or sufficient, to uniquely determine the fitting parameters. A reduction in the size of the basis is required and, hopefully, not all the quantities are important for the bulk phase relaxations. Three assumptions are made about the dynamics. First is that the bending, vibrational, and torsional modes are too high in energy to substantially contribute to the motion. Thus they are ignored. The second assumption is that the radical can be thought of as a diatomic in its rotational angular momentum behavior since the carbons are much more massive than the hydrogen isotopes. Furthermore, the rotational angular momentum is assumed to be well represented by a single average magnitude J since this is large. As well, a multipole expansion in \mathbf{J} is carried out and truncated at second order. Finally, the third assumption about the free evolution is that the proton spins may be ignored since the largest coupling of the muon spin is to the electron's spin. However, even with these three assumptions, the operator basis set used in the following for the full spin dynamics is 95 dimensional. The spin Hamiltonian for the radical is constructed from the angular momenta \mathbf{S} , \mathbf{J} , and \mathbf{I} , and the external magnetic field \mathbf{B} , as

$$H/\hbar = \omega_e \hat{\mathbf{B}} \cdot \mathbf{S} - \omega_\mu \hat{\mathbf{B}} \cdot \mathbf{I} + \omega_0 \mathbf{S} \cdot \mathbf{J} - \omega_J \hat{\mathbf{B}} \cdot \mathbf{J} + \omega_{SR} \mathbf{S} \cdot \mathbf{J} + \omega_{IR} \mathbf{I} \cdot \mathbf{J} + c_A \mathbf{I} \cdot [\mathbf{J}]^{(2)} \mathbf{S}. \quad (6)$$

As stated above, this Hamiltonian assumes that only up to second order effects in \mathbf{J} are important. The first three terms in this Hamiltonian form the standard muonium or hydrogen spin Hamiltonian which have well-known analytic eigenvalues and eigenvectors [8].

The last category of assumptions deals with the many-body interactions between the radical and the rest of the gas in the experimental chamber. It is assumed that only binary collisions are important so that a quantum (linearized) Bolt-

zmann equation [9–11] will accurately describe the dynamics of the gaseous system. Furthermore, it is assumed that the effect of the collisions between the radical and the other gas molecules is to relax only the rotational angular momentum of the radical. As this is coupled to the electron and muon spin angular momenta, the latter are also expected to relax. Neither the electron spin nor muon spin is directly relaxed by the collisions since they are only indirectly coupled to the geometrical shape of the free radical. Finally, since the observable of interest is the spin of the muon \mathbf{I} the translational degrees of freedom may be averaged over, see, for example, Ref. [12], to obtain the evolution equation

$$\begin{aligned} \frac{\partial \rho(t)}{\partial t} &= -i\mathcal{L}\rho(t) - \mathcal{R}\rho(t) \\ &= -\mathcal{G}\rho(t) \end{aligned} \quad (7)$$

for the spin-density operator $\rho(t)$. The time dependence is determined by the motion generator

$$\mathcal{G} = \mathcal{R} + i\mathcal{L}, \quad (8)$$

which consists of the free motion commutator (Liouville superoperator) of the spin Hamiltonian H ,

$$\mathcal{L}A \equiv \frac{1}{\hbar} [H, A]_-, \quad (9)$$

and the collision superoperator \mathcal{R} , which describes the relaxation due to collisions with molecules of the moderating gas. Consistent with the assumption that the translational degrees of freedom are in equilibrium and thus have been averaged over, \mathcal{R} will involve equilibrium averaged collision cross sections. The major effect of \mathcal{R} , which is rotationally invariant, is to cause the rotational angular momentum \mathbf{J} of the radical to decay to thermal equilibrium. Details of collision superoperators are given, for example, in Refs. [9–11] and [13–15]. For a given free Hamiltonian and an assumed form for the collision superoperator it is then a matter of solving Eq. (7) for the time evolution of the density operator. Such an approach has previously been used in studies of the hydrogen-atom isotope spin relaxation via electron-spin exchange [13], in gas phase NMR [14,16], in muon charge exchange processes [12], and in Muonium addition reactions [17].

Section II deals with the operator basis for the full spin system, and its restrictions for longitudinal and transverse relaxation phenomena. The basis elements are vector valued quantities since it is the muon spin angular momentum vector \mathbf{I} , that is observed. To classify the expansions, irreducible Cartesian tensor operators [18] (under the three-dimensional rotation group) [19–21] and standard Clebsch-Gordan couplings are used. Section III relates the experimental longitudinal signal Eq. (2) to the component of the muon spin in the magnetic-field direction using the longitudinal eigenvalues and eigenvectors of the motion generator Eq. (8), within the longitudinal basis Eq. (15). In general there will be more than one exponential contributing to the signal depending upon the specific dynamics. Section IV does the same for the transverse signal by relating the experimental result Eq. (3) to the transverse eigenvalues using the transverse basis Eq.

(26). Finally, Sec. V gives the results of fits to the transverse data and of the global fits to both the transverse and longitudinal data.

II. OPERATOR BASES

As the observed quantity is the muon spin angular momentum vector \mathbf{I} , a general basis describing the motion of this vector should be a vector valued basis. Both the longitudinal and transverse configurations are included in this general description and either one can be extracted using a reduction to the particular scalar component of the motion being observed. For example, the longitudinal signal is the component of the expectation value of the muon spin in the field direction while the transverse signal may be expressed as the (real part of the) positively rotating component in the plane perpendicular to the magnetic-field direction. In this way, the longitudinal and transverse bases are scalar valued bases.

Since the spin-density operator $\rho(t)$ is a function of the three spin vectors $\mathbf{I}, \mathbf{S}, \mathbf{J}$, and the field direction (unit vector) $\hat{\mathbf{B}}$, it is appropriate to use an orthonormal vector valued operator basis involving these quantities. Such a basis is described in Ref. [5] and is given in Cartesian tensor form as

$$\begin{aligned} \chi_M = & \sqrt{(2\alpha+1)(2\beta+1)} \mathcal{Y}^{(n)}(\mathbf{J}) \mathcal{Y}^{(m)}(\mathbf{S}) \\ & \times \odot^{m+n} \mathbf{V}(m, n, \alpha) \odot^\alpha \mathbf{V}(\alpha, \beta, r) \odot^r \mathcal{Y}^{(r)}(\hat{\mathbf{B}}) \\ & \times \odot^\beta \mathbf{V}(\beta, 1, p) \odot^p \mathcal{Y}^{(p)}(\mathbf{I}). \end{aligned} \quad (10)$$

The notation for irreducible Cartesian tensors $\mathcal{Y}^{(n)}$, n -fold tensor contraction $\odot^{(n)}$, and Clebsch-Gordan tensors $\mathbf{V}(m, n, \alpha)$, follows that of Coope and Snider [20,21]. This operator basis is orthonormal,

$$\langle\langle \chi_M | \chi_{M'} \rangle\rangle = \delta_{MM'} = \delta_{mm'} \delta_{nn'} \delta_{pp'} \delta_{\alpha\alpha'} \delta_{\beta\beta'} \delta_{rr'} \quad (11)$$

with respect to an inner product defined as follows:

$$\langle\langle \mathbf{Y} | \mathbf{Z} \rangle\rangle \equiv \frac{1}{4\pi(2I+1)(2S+1)(2J+1)} \text{Tr}_{I,S,J} \int d\hat{\mathbf{B}} \mathbf{Y}^\dagger \cdot \mathbf{Z}. \quad (12)$$

When the reduction to longitudinal and transverse components is performed, there is no longer a need for the vector dot product and the inner product

$$\langle\langle Y | Z \rangle\rangle \equiv \frac{1}{4\pi(2I+1)(2S+1)(2J+1)} \text{Tr}_{I,S,J} \int d\hat{\mathbf{B}} Y^\dagger Z \quad (13)$$

is appropriate. With the assumptions made about the spin Hamiltonian and the retention of only second order in \mathbf{J} multipoles, this full vector basis is 95 dimensional. The index M , for the basis consists of the combination $mnp, \alpha\beta r$ where m, n, p represent, respectively, the tensorial order of the angular momenta \mathbf{S}, \mathbf{J} , and \mathbf{I} , r is the tensorial order of the magnetic-field direction, while α and β are angular momentum coupling indices. Matrix elements of the motion generator Eq. (8)

$$\begin{aligned} G_{MM'} = & \langle\langle \chi_M | \mathcal{G} | \chi_{M'} \rangle\rangle \\ = & \langle\langle \chi_M | i\mathcal{L} | \chi_{M'} \rangle\rangle + \frac{1}{\tau_M} \delta_{MM'}, \end{aligned} \quad (14)$$

are calculated using this basis. See Ref. [5] for specific details for both the spin Hamiltonian terms and the collision terms.

A. Longitudinal basis

Experiments are carried out in either a longitudinal or a transverse configuration, that is, with the magnetic field and the initial muon spin either collinear or perpendicular. Moreover, since the Hamiltonian has $C_{\infty v}$ symmetry about the field direction $\hat{\mathbf{B}}$, the dynamics of the spin system separates into independent longitudinal and rotating components. Thus it is appropriate to restrict the general basis to bases appropriate for describing either the longitudinal or rotating dynamics. Matrix elements of the motion generator \mathcal{G} may then be determined from the full vector basis elements Eq. (14), using the appropriate set of restriction coefficients. The 35 dimensional real, scalar valued orthonormal longitudinal basis

$$\begin{aligned} \Phi_N^L = & \sqrt{2\alpha+1} \mathcal{Y}^{(n)}(\mathbf{J}) \mathcal{Y}^{(m)}(\mathbf{S}) \odot^{m+n} \mathbf{V}(m, n, \alpha) \\ & \times \odot^\alpha \mathbf{V}(\alpha, p, q) \odot^{p+q} \mathcal{Y}^{(q)}(\hat{\mathbf{B}}) \mathcal{Y}^{(p)}(\mathbf{I}) \end{aligned} \quad (15)$$

has been described previously [5]. Its numerical index N is to classify, in some convenient order, the set of parameters $mnp, \alpha q$. This scalar valued basis can be expanded in terms of the full vector valued basis χ_M according to

$$\Phi_N^L = \sum_{M=1}^{95} a_{M,N} \chi_M \cdot \hat{\mathbf{B}}. \quad (16)$$

The expansion coefficients are obtained [5] by using the orthonormality of the χ_M 's, whose use requires that Φ_N^L must be embedded as a vector in the same space as the χ_M , specifically that

$$\begin{aligned} a_{M,N} = & \langle\langle \chi_M | \Phi_N^L \hat{\mathbf{B}} \rangle\rangle = \langle\langle \chi_{mnp\alpha\beta r} | \Phi_{mnp\alpha q}^L \hat{\mathbf{B}} \rangle\rangle \\ = & (-1)^{\alpha+\beta+q+1} \left[\frac{(2\beta+1)(q+r+1)}{2} \right]^{1/2} \\ & \times \left\{ \begin{array}{ccc} \alpha & \beta & r \\ 1 & q & p \end{array} \right\} \delta_{|q-r|,1}. \end{aligned} \quad (17)$$

Note that only the q and r indices differ between the index sets N and M . Matrix elements of the motion generator Eq. (8) in the longitudinal basis

$$G_{NN'}^L = \langle\langle \Phi_N^L | \mathcal{G} | \Phi_{N'}^L \rangle\rangle = \sum_{M=1}^{95} \sum_{M'=1}^{95} a_{M,N}^* G_{MM'} a_{M',N'}, \quad (18)$$

can then be calculated from the full basis matrix elements $G_{MM'}$ Eq. (14). The explicit (numerical) solution of the spin evolution is to be solved by finding the complex eigenvalues λ_N^L and eigenvectors φ_N^L of \mathcal{G}^L ,

$$\mathcal{G}^L \varphi_N^L = \lambda_N^L \varphi_N^L. \quad (19)$$

These are determined numerically in terms of the longitudinal basis

$$\varphi_N^L = \sum_{M=1}^{35} c_{M,N}^L \Phi_M^L. \quad (20)$$

The association of a numerical index N to the sets of parameters $mnp, \alpha q$ is chosen in this work so that the first five operators in the longitudinal basis correspond to the muonium observables, that is, the first is the component of the muon spin in the longitudinal direction

$$\Phi_1^L = \Phi_{001,01}^L = 2\hat{\mathbf{B}} \cdot \mathbf{I}, \quad (21)$$

the second is the component of the electron spin in the longitudinal direction

$$\Phi_2^L = \Phi_{100,11}^L = 2\hat{\mathbf{B}} \cdot \mathbf{S}, \quad (22)$$

the third is the dot product between the electron and muon spins

$$\Phi_3^L = \Phi_{101,10}^L = \frac{4}{\sqrt{3}} \mathbf{S} \cdot \mathbf{I}, \quad (23)$$

the fourth is the component of the cross product between the electron and muon spins in the longitudinal direction

$$\Phi_4^L = \Phi_{101,11}^L = \sqrt{2} \hat{\mathbf{B}} \cdot (\mathbf{S} \times \mathbf{I}), \quad (24)$$

and the fifth is the symmetric traceless component of the tensor product of the electron and muon spins aligned along the field direction

$$\Phi_5^L = \Phi_{101,12}^L = 2\sqrt{6} \hat{\mathbf{B}} \cdot [\mathbf{SI}]^{(2)} \cdot \hat{\mathbf{B}}. \quad (25)$$

It is only the first element of this set whose expectation value is measured experimentally.

B. Transverse basis

For rotational ($C_{\infty v}$) symmetry, a right-handed (complex) three-dimensional coordinate system may be constructed from the magnetic-field direction $\hat{\mathbf{B}} = \hat{\mathbf{z}}$, the positively rotating unit vector $\hat{\mathbf{e}}_+ = (\hat{\mathbf{x}} + i\hat{\mathbf{y}})/\sqrt{2}$, and the negatively rotating unit vector $\hat{\mathbf{e}}_- = (\hat{\mathbf{x}} - i\hat{\mathbf{y}})/\sqrt{2}$. Thus to construct an orthonormal scalar valued transverse field basis set, the component with the positively rotating unit vector may be used, that is,

$$\begin{aligned} \Psi_N^T &= (2q+3) \left[\frac{2(2\alpha+1)}{q+2} \right]^{1/2} \mathcal{Y}^{(n)}(\mathbf{J}) \mathcal{Y}^{(m)}(\mathbf{S}) \\ &\times \odot^{m+n} \mathbf{V}(m, n, \alpha) \odot^{\alpha} \mathbf{V}(\alpha, p, q+1) \odot^{q+1} \\ &\times \mathbf{V}(q+1, 1, q) \odot^{q+1+p} \mathcal{Y}^{(q)}(\hat{\mathbf{B}}) \hat{\mathbf{e}}_+ \mathcal{Y}^{(p)}(\mathbf{I}). \quad (26) \end{aligned}$$

This complex basis set is 30 dimensional, whose numerical index N is associated with some convenient ordering of the $mnp, \alpha q$ parameter set having orthonormality expressed through the inner product of Eq. (13), that is,

$$\langle \langle \Psi_N^T | \Psi_{N'}^T \rangle \rangle = \delta_{NN'} = \delta_{mm'} \delta_{nn'} \delta_{pp'} \delta_{\alpha\alpha'} \delta_{qq'}. \quad (27)$$

Note that the negatively rotating transverse field basis set is just the complex conjugate of the above basis set, so only one set is needed in order to determine everything about the transverse system, but of course it is the rotating basis sets that describe the dynamically independent parts of the spin system. The positively rotating basis set may be expanded in terms of the full basis set Eq. (10) according to

$$\Psi_N^T = \sum_{M=1}^{95} b_{M,N} \chi_M \cdot \hat{\mathbf{e}}_+. \quad (28)$$

As for the longitudinal basis set expansion, the expansion coefficients are obtained by using the orthonormality of the χ_M , which requires embedding the scalar Ψ_N^T in the vector space in which χ_N is defined. This results in the expansion coefficients being given by

$$\begin{aligned} b_{M,N} &= \langle \langle \chi_M | \Psi_N^T \hat{\mathbf{e}}_- \rangle \rangle = \langle \langle \chi_{mnp\alpha\beta r} | \Psi_{mnp\alpha q} \hat{\mathbf{e}}_- \rangle \rangle \\ &= (-1)^{\alpha+\beta+q} \left[\frac{2\beta+1}{2(q+2)} \right]^{1/2} (2q+3) \\ &\times \begin{Bmatrix} r & 1 & q+1 \\ p & \alpha & \beta \end{Bmatrix} \\ &\times \left[\delta_{qr} \left(\frac{q+2}{2q+3} \right) - \delta_{r(q+2)} \frac{\sqrt{(q+2)(q+1)}}{2q+3} \right. \\ &\left. + i \delta_{r(q+1)} \left(\frac{q+2}{2q+3} \right)^{1/2} \right], \quad (29) \end{aligned}$$

with only the r and q indices differing in the two parameter sets. Matrix elements of the motion generator Eq. (8) in the transverse basis are then obtained according to

$$G_{NN'}^T = \langle \langle \Psi_N^T | \mathcal{G} | \Psi_{N'}^T \rangle \rangle = \sum_{M=1}^{95} \sum_{M'=1}^{95} b_{M,N}^* G_{MM'} b_{M',N'} \quad (30)$$

from the full basis matrix elements $G_{MM'}$, Eq. (14). The dynamical properties of the spin system in a transverse field can then be expressed in terms of the complex eigenvalues λ_N^T and eigenvectors φ_N^T of \mathcal{G}^T ,

$$\mathcal{G}^T \varphi_N^T = \lambda_N^T \varphi_N^T. \quad (31)$$

The latter are determined numerically as sets of expansion coefficients $c_{M,N}^T$ in terms of the transverse basis

$$\varphi_N^T = \sum_{M=1}^{30} c_{M,N}^T \Psi_M^T. \quad (32)$$

The indexing scheme was chosen so that the first four operators in the transverse basis correspond to the muonium observables. That is, the first is the component of muon spin which positively rotates in the plane perpendicular to the field direction

$$\Psi_1^T = \Psi_{001,00}^T = 2\mathbf{I} \cdot \hat{\mathbf{e}}_+, \quad (33)$$

the second is the component of electron spin which positively rotates in the plane perpendicular to the field direction

$$\Psi_2^T = \Psi_{100,10}^T = 2\mathbf{S} \cdot \hat{\mathbf{e}}_+, \quad (34)$$

the third is the positively rotating component of the cross product between the electron and muon spins

$$\Psi_3^T = \Psi_{101,10}^T = 2\sqrt{2}(\mathbf{S} \times \mathbf{I}) \cdot \hat{\mathbf{e}}_+, \quad (35)$$

and the fourth is a component of the symmetric traceless part of the tensor product of the electron and muon spins

$$\Psi_4^T = \Psi_{101,11}^T = 4\sqrt{2}\hat{\mathbf{B}} \cdot [\mathbf{SI}]^{(2)} \cdot \hat{\mathbf{e}}_+. \quad (36)$$

Experimental measurements involve the relaxation rate and oscillation frequency of the muon spin. Both these quantities are determined by the expectation value of Ψ_1^T .

III. OBSERVABLE LONGITUDINAL SIGNAL

The experiments carried out in longitudinal field detect the component of the muon spin in the magnetic-field direction, that is,

$$S_L(t) = \hat{\mathbf{B}}(\mathbf{I})(t) = \text{Tr}_I \hat{\mathbf{B}} \cdot \mathbf{I} \rho(t) = \langle \langle \Phi_1^L | \rho(t) \rangle \rangle. \quad (37)$$

By the $C_{\infty v}$ symmetry of the experimental setup, only the longitudinal basis contributes to this signal. Thus the time dependence is governed entirely by \mathcal{G}^L and conveniently expressed in terms of its eigenvalues and eigenfunctions, namely,

$$\begin{aligned} \rho(t) &= e^{-\mathcal{G}^L t} \rho(0) = \sum_{N=1}^{35} e^{-\mathcal{G}^L t} \varphi_N^L p_N^L(0) \\ &= \sum_{N=1}^{35} \varphi_N^L e^{-\lambda_N^L t} p_N^L(0). \end{aligned} \quad (38)$$

The observed signal Eq. (37) is thus a sum of complex exponentials and amplitudes,

$$\begin{aligned} S_L(t) &= \sum_{N=1}^{35} e^{-\lambda_N^L t} p_N^L(0) \langle \langle \Phi_1^L | \varphi_N^L \rangle \rangle \\ &= \sum_{N=1}^{35} e^{-\lambda_N^L t} p_N^L(0) c_{N1}^L = \sum_{N=1}^{35} e^{-\lambda_N^L t} A_N^L. \end{aligned} \quad (39)$$

On the basis that at the zero of time, only the muon spin is out of equilibrium and that this spin is pointed in the $\hat{\mathbf{B}}$ direction, then it is to be shown that the amplitudes A_N^L are determined completely by the expansion coefficients of the eigenvectors in terms of the longitudinal operator basis. To start this demonstration, note that the initial expectation value for the muon spin component is 1/2, namely, $\langle \hat{\mathbf{B}} \cdot \mathbf{I} \rangle = 1/2$ with the consequence that the nonequilibrium (ne) part of the spin-density operator is

$$\rho^{\text{ne}}(0) = \hat{\mathbf{B}} \cdot \mathbf{I} = \frac{1}{2} \Phi_1^L = \sum_{N=1}^{35} \varphi_N^L p_N^L(0). \quad (40)$$

This sum over the eigenvectors needs to be inverted in order to identify the expansion coefficients $p_N^L(0)$. Since the motion generator \mathcal{G}^L is not Hermitian, nor even necessarily normal, the eigenvectors are not necessarily orthogonal. Thus the inversion requires the use of the eigenvector overlap matrix

$$O_{NN'}^L \equiv \langle \langle \varphi_N^L | \varphi_{N'}^L \rangle \rangle = \sum_{M=1}^{35} c_{NM}^{L*} c_{N'M}^L. \quad (41)$$

In this way, the expansion coefficients $p_N^L(0)$ are calculated to be

$$\begin{aligned} p_N^L(0) &= \sum_{N'=1}^{35} [(O^L)^{-1}]_{NN'} \langle \langle \varphi_{N'}^L | \rho^{\text{ne}}(0) \rangle \rangle \\ &= \frac{1}{2} \sum_{N'=1}^{35} [(O^L)^{-1}]_{NN'} c_{N'1}^{L*} \end{aligned} \quad (42)$$

while the amplitudes of the signal are

$$A_N^L = \frac{1}{2} \sum_{N'=1}^{35} c_{N1}^L [(O^L)^{-1}]_{NN'} c_{N'1}^{L*}. \quad (43)$$

If the eigenvectors actually are orthonormal, this sum reduces to give $A_N^L = \frac{1}{2} |c_{N1}^L|^2$.

The complex eigenvalues

$$\lambda_N^L = \left(\frac{1}{T_{1N}} \right) + i\omega_N^L \quad (44)$$

are usually expressed in terms of relaxation times T_{1N} , and frequencies ω_N^L . For longitudinal signals, some of these will have zero frequency and the signal becomes

$$\begin{aligned} S_L(t) &= \sum_{N \ni \omega_N^L = 0} e^{-t/T_{1N}} A_N^L \\ &+ \sum_{N \ni \omega_N^L \neq 0} e^{-t/T_{1N}} \cos(\omega_N^L t + \theta_N^L) |A_N^L| \end{aligned} \quad (45)$$

since for each term with frequency ω_N^L there is a corresponding term with frequency $-\omega_N^L$ and complex conjugate amplitude. In carrying out the experiments, the nonzero frequencies are found to be too large to be measured so that the signal is then simply given by the zero-frequency components,

$$S_L(t) = \sum_{N \ni \omega_N^L = 0} e^{-t/T_{1N}} A_N^L. \quad (46)$$

In general there may be a number of modes which contribute to the observed signal which may cause fitting problems for the experimental measurements and for the theoretical description of them. Thus the assumed form for the experimental longitudinal signal Eq. (2) may not be appropriate in all cases. That is, there may be some fields and pressures where only a single mode is populated and others where two or more modes contribute. Care must be taken both in carrying out the experiments and in their theoretical interpretation to ensure that these various situations are treated properly.

For pure muonium there are five longitudinal modes, of which three have zero frequency. Thus there could be up to three different exponentials and amplitudes if all the modes can be observed. For the present case of the C_2H_4Mu radical and under the current theoretical assumptions, there are 35 longitudinal modes. If only the linear terms in the rotational angular momentum are retained then there are only 15 longitudinal modes of which only a few will have zero frequency. It turns out, see Sec. V, that the retention of only the linear in \mathbf{J} terms in the Hamiltonian is sufficient for the interpretation of the C_2H_4Mu experiments.

IV. OBSERVABLE TRANSVERSE SIGNAL

The experiments carried out in transverse field detect the component of the muon spin which rotates in the plane perpendicular to the magnetic-field direction. Here this is analyzed according to the positively rotating component of the spin, that is,

$$S_+(t) = \hat{\mathbf{e}}_+ \cdot \langle \mathbf{I} \rangle(t) = \langle \langle \Psi_1^T | \rho(t) \rangle \rangle. \quad (47)$$

As with the longitudinal signal, this transverse result may be expressed as follows:

$$S_+(t) = \sum_{N=1}^{30} e^{-\lambda_N^T t} A_N^T, \quad (48)$$

where the amplitudes are the transverse analogs of the longitudinal amplitudes

$$A_N^T = \frac{1}{2} \sum_{N'=1}^{30} c_{N1}^T [(O^T)^{-1}]_{NN'} c_{N'1}^{T*}, \quad (49)$$

on the assumption that initially the spin was 100% in the positively rotating component.

The complex eigenvalues

$$\lambda_N^T = \left(\frac{1}{T_{2N}} \right) + i\omega_N^T \quad (50)$$

are usually expressed in terms of relaxation times T_{2N} and frequencies ω_N^T . For transverse signals, none of these have zero frequency so that the real part of the signal becomes a series of damped cosines,

$$S_T(t) = \text{Re} S_+(t) = \sum_{N=1}^{30} e^{-t/T_{2N}} \cos(\omega_N^T t + \theta_N^T) |A_N^T|. \quad (51)$$

In the ethyl radical experiments Eq. (3) only the lowest frequency is observed so that the measured signal

$$S_T(t) = e^{-t/T_2} \cos(\omega^T t + \theta^T) |A^T|. \quad (52)$$

involves only one decay rate $1/T_2$ and one frequency ω^T . This greatly simplifies any problems with regard to fitting the experimental data or its theoretical interpretation as both the frequency and the decay rate result from a single mode.

V. FITS TO EXPERIMENTAL DATA

Experiments have been performed [1–4] in both longitudinal and transverse fields. The collected experimental data have been fit to signals with single exponentials of the form of Eqs. (2) and (3). A fit [5] to the longitudinal T_1 data using the current theory has been made. In that fit it was assumed that only one mode contributes to all the longitudinal signals and that the choice of mode was the one with the smallest relaxation rate $1/T_{1N}$. The parameters obtained in this way were not well defined and their values did not necessarily fall within the ranges expected on the basis of other arguments. It was recognized that there was a difficulty with the interpretation of the longitudinal data, specifically which particular relaxation mode, or more generally, modes, contribute to the signal. From an experimental point of view this is a question of whether the collected data is to be fit to a single exponential or to more than one exponential. The difficulty is that there may be large ranges of fields and/or pressures where there is only one mode and small ranges where more than one mode contributes. As well there may be cases where two modes contribute but that they can not be differentiated in the fitting process. From a theoretical point of view, it should not be assumed that only one mode contributes and that it is the one with the slowest relaxation rate. To answer these questions, it is appropriate to calculate the mode amplitudes and to consider only those modes with appreciable amplitude. Since these difficulties do not exist for the transverse signal [since there is then an observed frequency which aids in the selection of which (transverse) mode is being observed] it is more appropriate to first fit the transverse signal and then use the Hamiltonian parameters and collision times deduced therefrom to either attempt to fit all sets of data at once or to predict the longitudinal (T_1) data.

A. Transverse relaxation fitting

In transverse fields, the signal has a damped cosine behavior Eq. (3) with a single relaxation rate. Neither the theory nor the experiments require more than one relaxation rate per frequency. Such a situation might occur if two frequencies were sufficiently close and agreed with the observed frequency, as is the case for very low magnetic fields. However, the fields in the experiments were quite high. The experimental data [1–4] consist of 34 measured relaxation rates with their corresponding frequencies, for pressures ranging from 1.0 to 14.6 atmospheres and in fields from 9.5 to 26.6 kG.

The theory presented here is capable of predicting both relaxation rates and frequencies. This is very important for the theory since the frequencies are extremely sensitive to the size of the isotropic hyperfine constant ω_0 . Indeed, in the fitting, the value of ω_0 is always very close to 2073 rad/ μ sec, which is the frequency measured in transverse field experiments [22]. The contributions to the total χ^2 per degree of freedom (χ^2) from the frequencies are negligible in all fits, with the relaxation rates contributing virtually all the uncertainty. Since the phenomenological approach [1–4] does not involve fitting the frequency, the χ^2 reported for the present theory are those for the relaxation rate only.

The phenomenological approach represents the relaxation rate in a form of the type

TABLE I. Phenomenological transverse parameters.

Parameter	Value	Error
Δ_{EP} (rad/ μ s)	1661	309
Δ_M (rad/ μ s)	279	75.5
τ (ps/atm)	81.8	49.8
χ^2	1.73	

$$\frac{1}{T_2} = 2\Delta_{EP}^2 \left[\frac{\tau}{1 + (\omega_e \tau)^2} \right] + 2\Delta_M^2 \left[\frac{\tau}{1 + (\omega_\mu \tau)^2} \right], \quad (53)$$

where Δ_{EP} , Δ_M , and τ are fitting parameters. See Refs. [1–4] for a detailed discussion of the meanings of these quantities. In order to provide a comparison for the present theoretical approach, the experimental data was fit to Eq. (53). The results of this fit are reported in Table I with a χ^2 of 1.73. The three parameters were found to be well defined and the addition of the experimental stopping distribution parameter η_0 , see Eq. (5), was not required. Although the addition of this parameter in a fit produces a slightly better χ^2 , the parameter is not well defined.

Under the assumptions in the current theoretical approach, there are five radical fitting parameters, γ_J , ω_0 , ω_{SR} , ω_{IR} , and c_A , two collisional parameters τ_1 and τ_2 , and one experimental parameter η_0 , see Eq. (5). In all the theoretical fits the value of the magnitude J of the rotational angular momentum \mathbf{J} , has been taken to be 17 since this is its thermal average value. When this value is altered only the coupling parameters that depend upon it change in size in a predictable manner. The theoretical parameters fall into three categories depending upon their relation to the tensorial order of the rotational angular momentum \mathbf{J} . Only the isotropic hyperfine coupling parameter ω_0 between the electron and muon spins is independent of \mathbf{J} . It is this parameter which dictates the observed frequency and it is well defined in all the fits. Although it is recorded as a fitting parameter, it is not free to vary with respect to the relaxation rates and should not be considered as a fitting parameter for the relaxation rates. The Hamiltonian has both linear and quadratic in

TABLE II. Theoretical transverse parameters.

Parameter	Value	Error
ω_o (rad/ μ s)	2073	16
ω_{sr} (rad/ μ s)	-233	43
ω_{ir} (rad/ μ s)	28.0	7.3
τ_1 (ps/atm)	82.2	48.8
χ^2	1.75	

\mathbf{J} terms. If only the linear in \mathbf{J} terms are kept, then the spin system is parameterized by the two spin-rotation parameters ω_{SR} and ω_{IR} , the rotational gyromagnetic ratio γ_J , and the collision lifetime τ_1 . The quadratic in \mathbf{J} terms add as parameters the anisotropic hyperfine coupling constant c_A and the collision lifetime τ_2 .

To fit the data, matrix elements of the motion generator Eq. (8) in the full basis are calculated and from these, the matrix elements Eq. (30) of the transverse motion generator is deduced using the restricting coefficients Eq. (29). Eigenvalues and eigenvectors of this matrix are obtained using standard numerical procedures, see for example, [24]. Signal amplitudes are determined using Eq. (49). To choose the correct mode, the modes with nonzero amplitude (defined as greater than 1% of the total amplitude) are selected and then the mode with the minimum absolute frequency is chosen. This selection procedure is that of the experiments, that is, of the populated modes the one with the lowest frequency is observed. Fits to the experimental T_2 data are performed using MINUIT [23]. For each pressure and field, new eigenvalues and eigenvectors must be calculated.

A good fit to the T_2 data, with a χ^2 of 1.75, was obtained keeping only the linear in \mathbf{J} terms in the Hamiltonian. This requires using only three fitting parameters, namely, ω_{SR} , ω_{IR} , and τ_1 , see Table II, since ω_0 is determined by the frequency dependence. That is, only the vector behavior of the rotational angular momentum was required to adequately fit the current experimental data with reasonably well defined parameters. Inclusion of any combination of the rotational gyromagnetic term, the second rank tensorial rotational an-

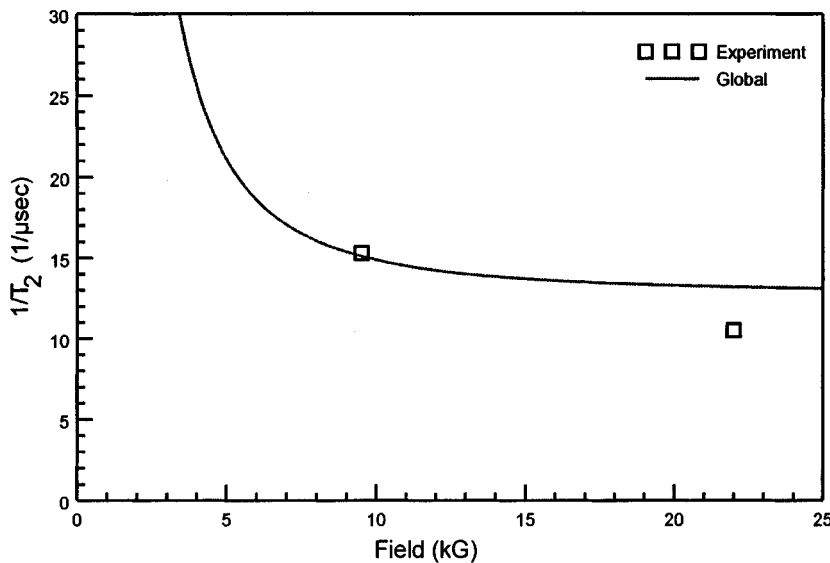


FIG. 1. Experimental transverse muon spin-relaxation rate vs magnetic field at a pressure of 1.0 atmosphere. The solid curve is the global fit while the squares are the experimental points.

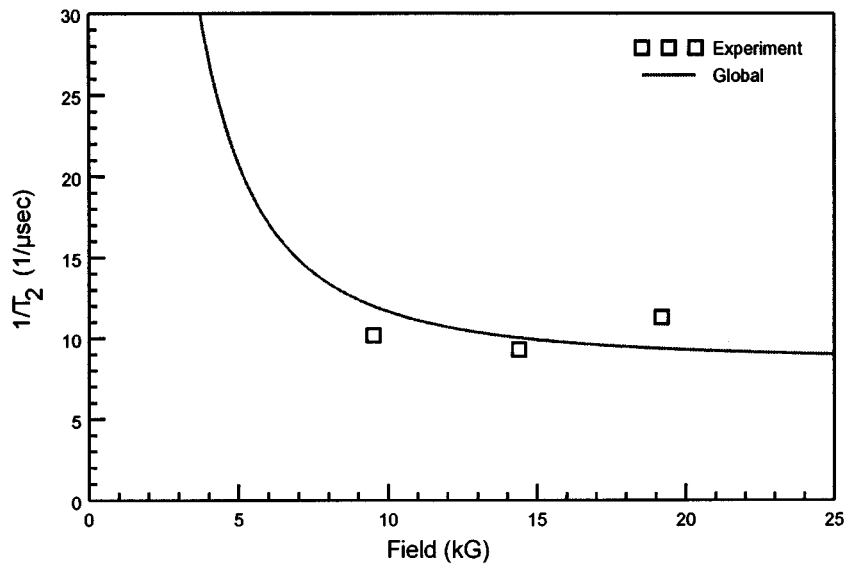


FIG. 2. Same as Fig. 1 but for a pressure of 1.5 atmospheres.

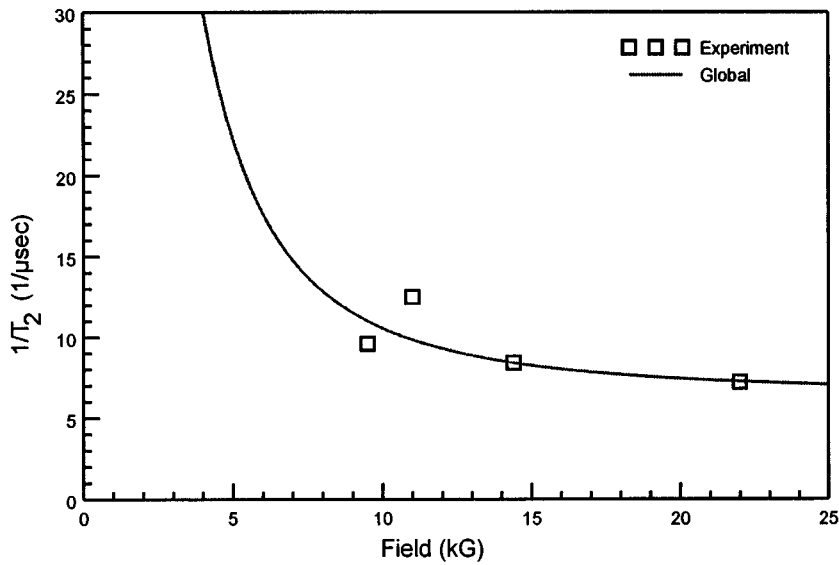


FIG. 3. Same as Fig. 1 but for a pressure of 2.0 atmospheres.

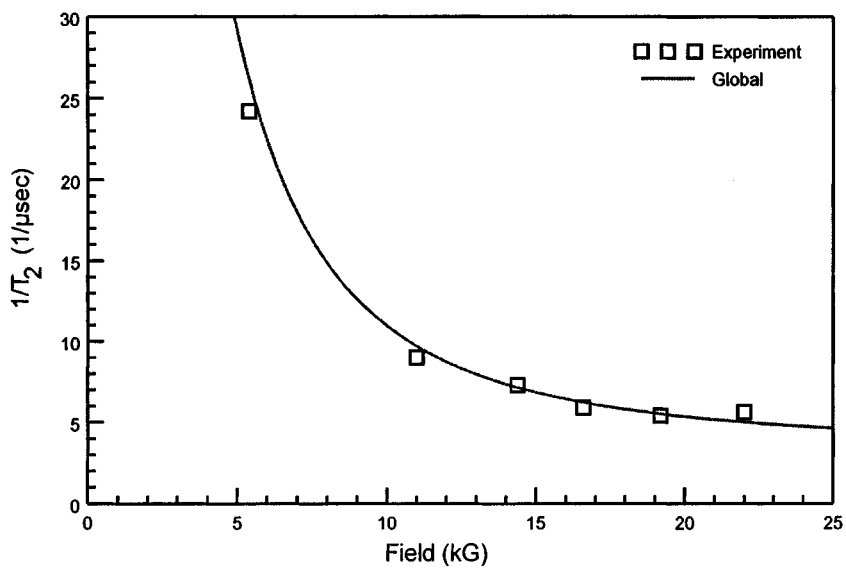


FIG. 4. Same as Fig. 1 but for a pressure of 3.8 atmospheres.

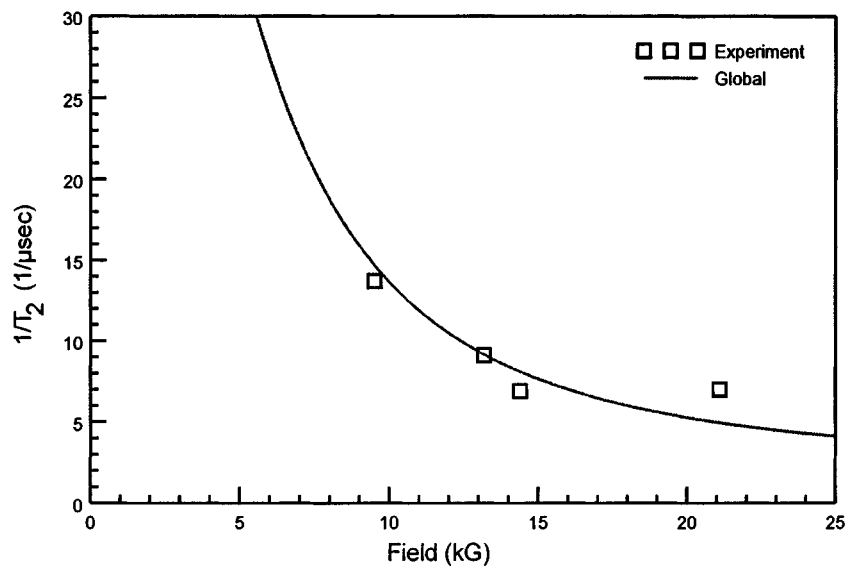


FIG. 5. Same as Fig. 1 but for a pressure of 6.5 atmospheres.

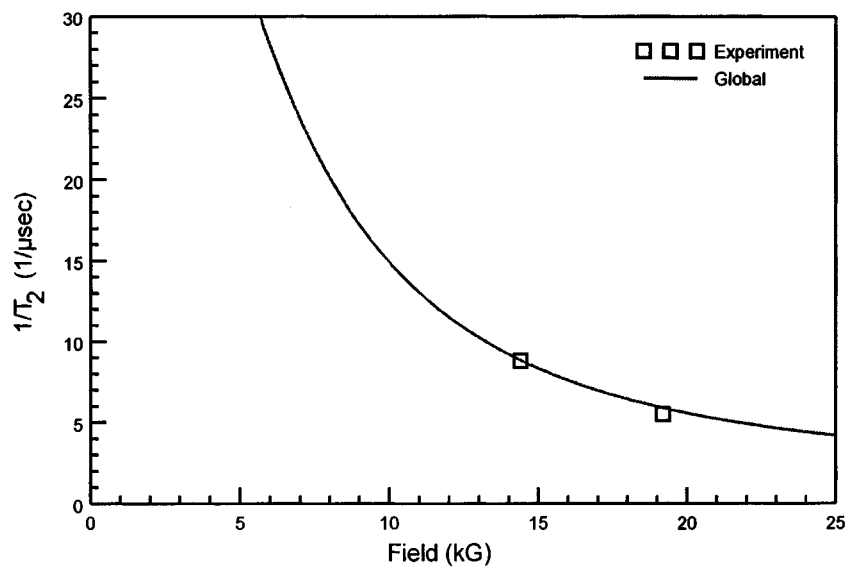


FIG. 6. Same as Fig. 1 but for a pressure of 8.0 atmospheres.

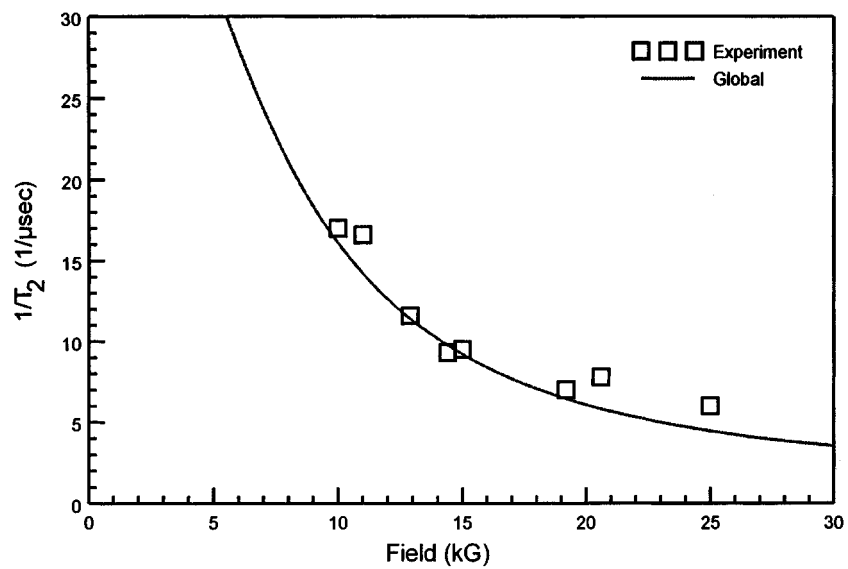


FIG. 7. Same as Fig. 1 but for a pressure of 10.0 atmospheres.

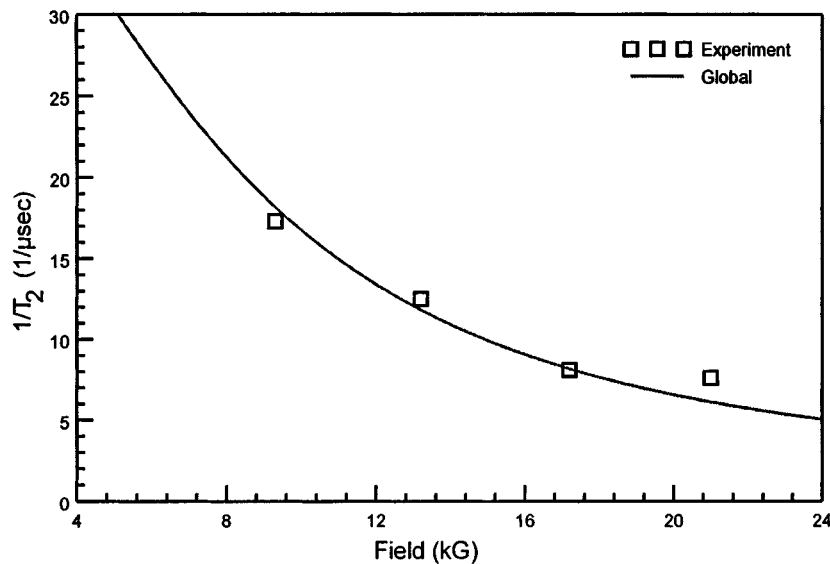


FIG. 8. Same as Fig. 1 but for a pressure of 11.9 atmospheres.

gular momentum contribution, and the experimental stopping distribution contribution η_0 , see Eq. (5), produced similar fits. However, the extra parameters were not well defined in these fits. This is similar to the phenomenological approach. Plots of the experimental data and the current theoretical fit are presented in Figs. 1–9. The transverse fits discussed here are virtually indistinguishable from the global fits which are given by the solid lines, see Sec. V B. Except at low fields the theoretical transverse, theoretical global and phenomenological fits are indistinguishable and, even for low fields, there is not much difference. While it is difficult to relate the molecular parameters ω_{SR} and ω_{IR} to the phenomenological parameters Δ_{EP} and Δ_M it seems reasonable to conclude that the lifetimes τ_1 and τ are comparable quantities.

B. Global fits and longitudinal relaxation

In longitudinal fields, the experimental time dependence has been fitted [1–4] with a single relaxation rate, see Eq. (2). However the theory suggests that there might be more than one relaxation rate. The experimental data [1–4] con-

sists of 56 relaxation rates for pressures ranging from 1.0 to 11.9 atmospheres and for fields from 0.5 to 35.0 kG.

The phenomenological approach represents the relaxation rate in a form of the type

$$\frac{1}{T_1} = 4[\Delta_E^2 + x^2\Delta_{ME}^2] \left[\frac{1}{1+x^2} \right] \left[\frac{\tau}{1+(\omega_e\tau)^2} \right] + 2\Delta_M^2\tau, \quad (54)$$

where $x=B/B_0$ and $B_0=\omega_0/(\gamma_e+\gamma_\mu)=118$ G with $\omega_0=2073$ rad/ μ sec and Δ_E , Δ_{ME} , Δ_M , and τ are four fitting parameters. For global fits to both the longitudinal and transverse data, the parameter Δ_{EP}^2 in the transverse fit is set equal to $\Delta_E^2 + \Delta_{ME}^2$. A fit to both the longitudinal and transverse data using Eqs. (53) and (54) was made with a resulting χ^2 of 10.40. The contribution to χ^2 from the longitudinal data was 2.96 while the contribution from the transverse data was 7.44. For the transverse data the χ^2 was mainly due to the predicted low pressure $1/T_2$ values being too small. Since the effect of the transverse signal experimental parameter,

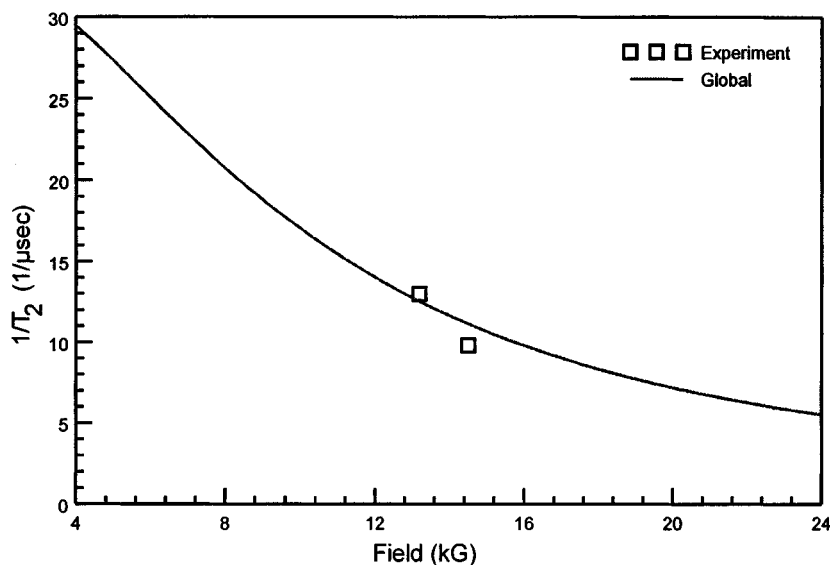


FIG. 9. Same as Fig. 1 but for a pressure of 14.6 atmospheres.

TABLE III. Phenomenological global parameters.

Parameter	Value	Error
Δ_E (rad/ μ s)	1511	143
Δ_{ME} (rad/ μ s)	232	13
Δ_M (rad/ μ s)	22.8	16.4
τ (ps/atm)	63.8	8.5
η_0 (atm/ μ s)	12.4	4.5
χ^2	3.05	

TABLE IV. Theoretical global parameters.

Parameter	Value	Error
ω_o (rad/ μ s)	2074	25
ω_{sr} (rad/ μ s)	-178	31
ω_{ir} (rad/ μ s)	21.9	3.1
τ_1 (ps/atm)	150	25
γ_J (rad/ μ s G)	-1.18	0.29
η_0 (atm/ μ s)	5.42	4.85
χ^2	3.07	

η_0 , is greatest at low pressures, a fit was also made including this term with parameters given in Table III. The resulting χ^2 was 3.05 with a $1/T_1$ contribution of 2.29 and a $1/T_2$ contribution of 0.756. The values of the fitting parameters reported here differ slightly from those given in Refs. [1–4] due to variations in the details of the phenomenological equations used and the available experimental data. Clearly the fitting to the longitudinal data is slightly improved whereas the transverse part of the fit is greatly improved. Thus the phenomenological approach gives a global fit to both longitudinal and transverse signals with five fitting parameters.

To fit the data with the current theoretical approach, matrix elements of the motion generator Eq. (8) in the full basis are calculated. Then using the restricting coefficients, Eq. (17), to relate the full and longitudinal bases, the motion generator in the longitudinal basis is obtained Eq. (18). Eigenvalues and eigenvectors of this matrix are obtained. Signal amplitudes are determined using Eq. (43). To choose the correct mode, the modes with nonzero amplitude (defined as greater than 1% of the total amplitude) are selected and then sorted as to whether they have zero or nonzero frequency. The significantly populated zero-frequency mode with the minimum relaxation rate was chosen and this was selected as the single mode to be compared with the experimental T_1 since the experimental fitting was to a single exponential relaxation. For each pressure and field new eigenvalues and

eigenvectors must be calculated. The transverse field data was fit in the manner discussed in Sec. V A.

The transverse field fitting parameters were used as a starting point to attempt a global fit to all the transverse and longitudinal data simultaneously. With only the four parameters that were well defined by the transverse fit it was not possible to find an acceptable global fit. However, when the rotational angular momentum gyromagnetic term γ_J was included, a not unreasonable global fit was obtained. This fit has a χ^2 of 4.23 with a $1/T_1$ contribution of 2.61 and a $1/T_2$ contribution of 1.62. It is comparable to the fit obtained using the phenomenological approach with no correction for stopping distribution. An even better fit resulted when the experimental stopping distribution parameter η_0 was included, see Table IV. The χ^2 is 3.07 with contributions of 2.41 from $1/T_1$ and 0.655 from $1/T_2$. In this case the longitudinal fits are slightly improved while the transverse fits have been appreciably improved. As with the phenomenological approach there are five fitting parameters for the relaxation rates with the isotropic hyperfine parameter ω_0 fit by the frequency. Plots of the theoretical global fit to the transverse data are given by the solid lines in Figs. 1–9 while plots of the theoretical global fit and the longitudinal data are given in Figs. 10–15.

If the inclusion of the experimental stopping distribution

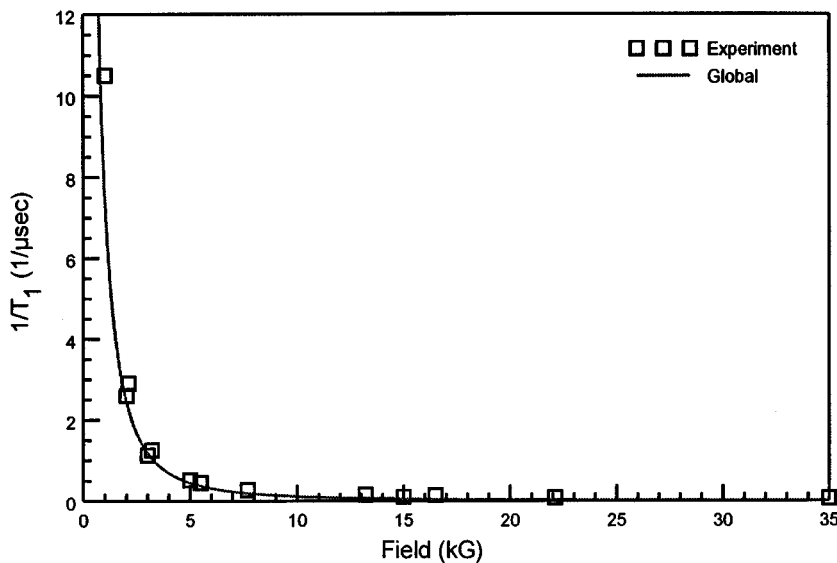


FIG. 10. Experimental longitudinal muon spin-relaxation rate vs magnetic field at a pressure of 1.0 atmosphere. The solid curve is the global fit obtained while the squares are the experimental data points.

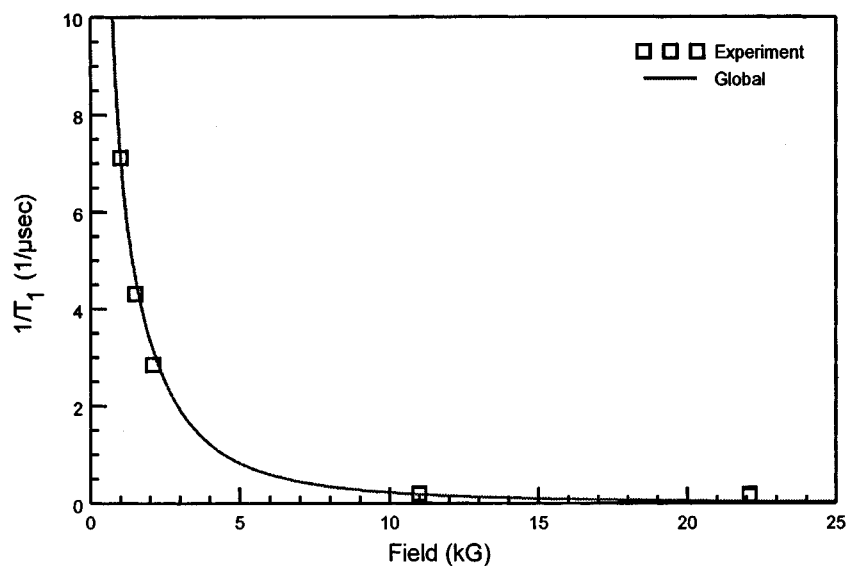


FIG. 11. Same as Fig. 10 but for a pressure of 2.0 atmospheres.

term is valid, then the resulting fits to η_0 should agree within experimental error between the two fits. This is the case as the phenomenological fit produces 12.4 ± 4.5 atm/ μ s while the theoretical fit gives 5.42 ± 4.85 atm/ μ s. It is to be noted that at the lowest pressures, namely 1.0 and 1.5 atm, that it is the relaxation associated with this stopping distribution that is the dominant part of the observed relaxation rate.

VI. DISCUSSION

A theoretical study of the muon spin relaxation of the gaseous C_2H_4Mu radical has been extended to transverse fields. Fits to the transverse field data by itself were obtained as were global fits to both the transverse and longitudinal data. These fits give very good representations of the experimentally reported relaxation rates T_1 and T_2 . Fits based on phenomenological formulas are of comparable accuracy. The theoretical treatment has the advantage that it is expressed in terms of well defined molecular properties of the radical and collisional lifetimes.

The treatment given here is based on a quantum Boltzmann equation that incorporates the dynamics of the freely moving radical through a spin Hamiltonian, plus the decay to thermal equilibrium associated with collisions of the radical with other molecules in the gas. For application to spin relaxation, it has been assumed that only the direction of rotation of the radical is affected by such collisions since the intermolecular potential is not much influenced by the other out-of-equilibrium (angular momentum directions) degrees of freedom. The C_2H_4Mu radical has muon **I**, electron **S**, and four proton **I_H** spins as well as the rotational angular momentum **J**. Thus the spin Hamiltonian correctly should include all possible couplings between all these spins. The large gyromagnetic ratio of the electron implies that the electron spin is the leading contributor to coupling the muon and rotational angular momentum and to the effect of the applied magnetic field. Thus the electron spin must be carefully included. In practice, both to keep the computations within bounds, and also because there is only so much data to determine the associated coupling constants, a selection must

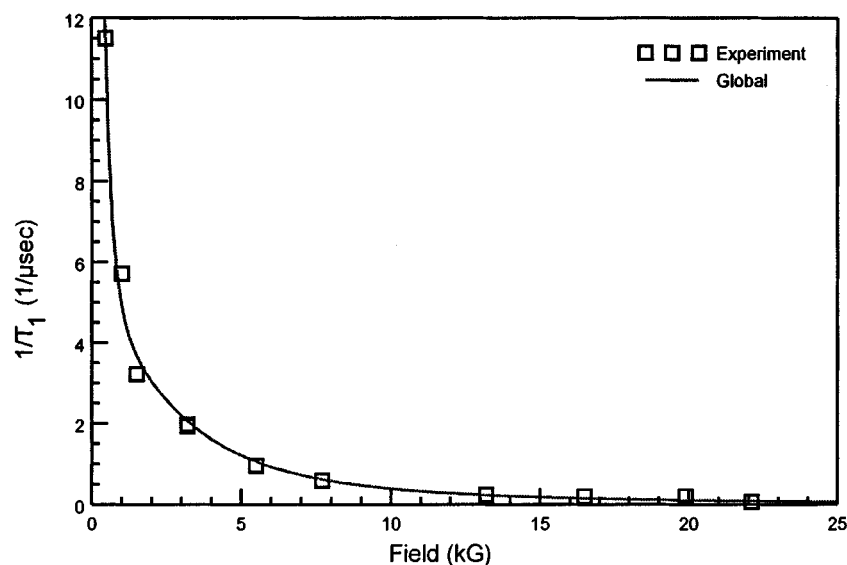


FIG. 12. Same as Fig. 10 but for a pressure of 3.8 atmospheres.

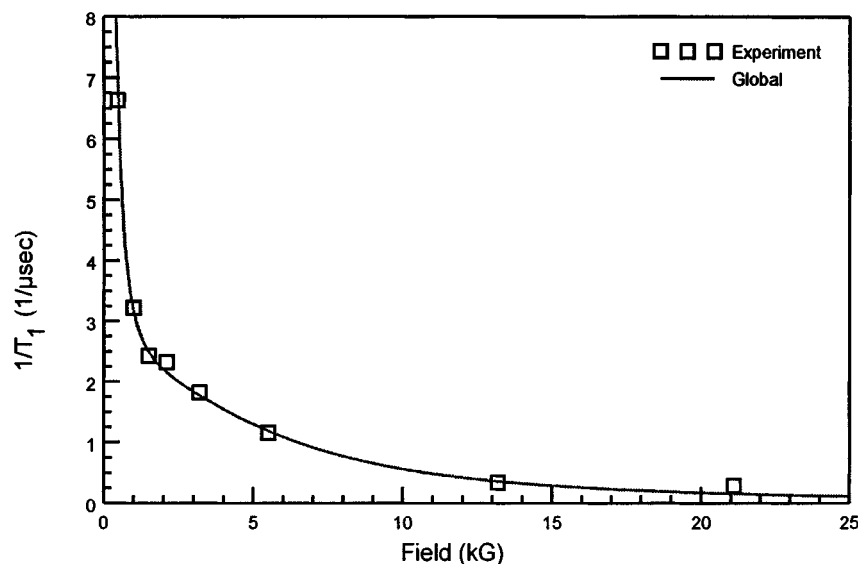


FIG. 13. Same as Fig. 10 but for a pressure of 6.5 atmospheres.

be made as to which terms in the Hamiltonian are important to include, and to which terms can be ignored. The first to go are the terms involving the proton spins, on the physical basis that the small proton gyromagnetic ratio should have only a very small direct effect on the measured muon spin, thus their major effect should only be via an indirect coupling through the electron spin. It would be nice to explore how much their presence would affect the measured muon spin relaxation rate, but since it is indirect, it has been assumed to be relatively unimportant and consequently ignored in the present treatment. Based on the (presumably) small gyromagnetic ratio associated with the radical's rotational (\mathbf{J}) motion, it is reasonable to expand the Hamiltonian in powers of \mathbf{J} . Note that the relatively large mass of the carbons has been used to assume that the radical can be treated as a diatomic. While the presence of quadratic terms in \mathbf{J} were explored, they were found to be unnecessary for an adequate fit of the data, and if they were included, the resulting values of the coupling constants were not well determined, nor was it clear that the fit was improved. That is, the

experimental data was not of sufficient accuracy or quantity, to give a unique determination of these coupling constants. Thus they were left out.

Even with the restrictions on the number of degrees of freedom discussed above, the linearized Boltzmann equation is still 19 dimensional for solving for the longitudinal muon spin relaxation, and 15 dimensional for the transverse. The eigenvectors for these sets of coupled linear equations are the precession-relaxation modes for the spin dynamics. It is then a question of which of the 19 (15) precession-relaxation modes is measured experimentally. Since the experimental data fits a simple exponential decay, one mode must dominate the relaxation. In our previous work [5] on the longitudinal relaxation it was assumed that it was the mode with the slowest relaxation rate that dominates. The resulting fit to the experimental data was reasonable but the fitting parameters that were obtained did not appear to be physically very reasonable. This was presumably due to the fitting procedure adjusting the parameters to make a best compromise to fit the experimental data with this fitting procedure. When attempt-

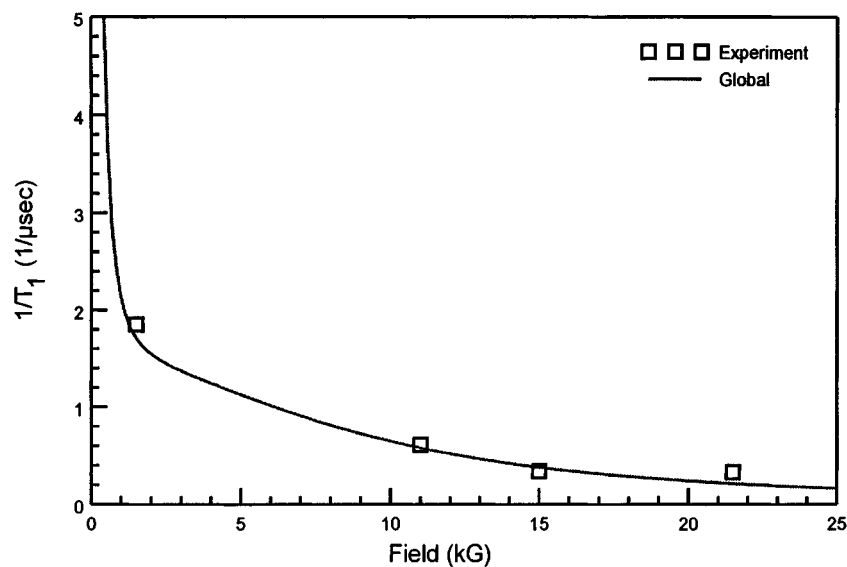


FIG. 14. Same as Fig. 10 but for a pressure of 10.0 atmospheres.

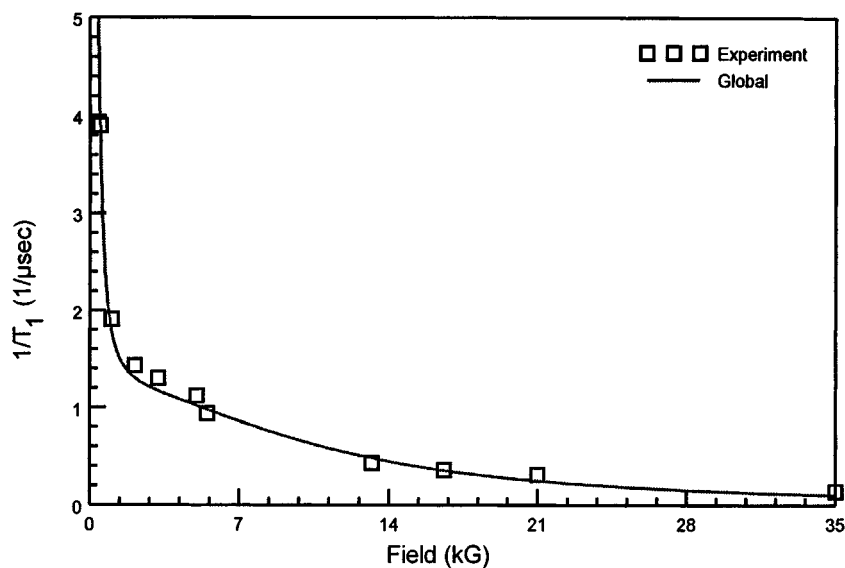


FIG. 15. Same as Fig. 10 but for a pressure of 11.9 atmospheres.

ing to fit the transverse relaxation rates, it was soon discovered that a different method of selection of precession-relaxation mode needs to be made. It was first considered necessary to find which mode has most of the amplitude of the muon spin. It is also important to ask how the modes are initially excited. In this work, the last question was answered by assuming that the experiments are carried out in such a way that there are no spin interactions before the radical is formed or until thermalization has occurred. That is, the initial state of the spins in the radical are assumed to be random except for the muon spin. If spin dynamic effects occurred prior to the thermalization of the radical, then the muon spin amplitude could be distributed among the other spins, in particular, with the electron spin. In such a case, a different

initial spin state would be appropriate, with the result that the populations of the different relaxation modes might be quite different. It is this selection of which mode is to dominate the relaxation that has led to the present much better fit of the experimental data.

ACKNOWLEDGMENTS

This work was supported in part by the Natural Sciences and Engineering Research Council of Canada. The authors thank Dr. Fleming, Dr. Arsenau, and Dr. Pan for access to the experimental data and for various discussions regarding the experiments.

-
- [1] D.G. Fleming, R.F. Kiefl, D.M. Garner, M. Senba, A.C. Gonzalez, J.R. Kempton, D.J. Arsenau, K. Venkateswaran, P.W. Percival, J.C. Brodovitch, S.K. Leung, D. Yu, and S.F.J. Cox, *Hyp. Int.* **65**, 767 (1990).
- [2] J.J. Pan, D.G. Fleming, M. Senba, D.J. Arsenau, R. Snooks, S. Baer, M. Shelley, P.W. Percival, J.C. Brodovitch, B. Addison-Jones, S. Wlodek, and S.F.J. Cox, *Hyp. Int.* **87**, 865 (1994).
- [3] J.J. Pan, PhD. thesis, University of British Columbia, 1995.
- [4] D.G. Fleming, J. J. Pan, M. Senba, D.J. Arsenau, R.F. Kiefl, M. Y. Shelly, S. F. J. Cox, P. W. Percival, and J.C. Brodovitch, *J. Chem. Phys.* (to be published).
- [5] R. E. Turner and R. F. Snider, *Phys. Rev. A* **50**, 4743 (1994).
- [6] D. G. Fleming, D. M. Garner, L. C. Vaz, D. C. Walker, J. H. Brewer, and K. M. Crowe, *Adv. Chem.* **175**, 279 (1979).
- [7] R. H. Heffner and D. G. Fleming, *Phys. Today* **37**, 2 (1984); E. Roduner, *The Positive Muon as a Probe in Free Radical Chemistry*, Vol. 49 of *Lecture Notes in Chemistry* (Springer-Verlag, Berlin, 1988); E. Roduner, *Chem. Soc. Rev.* **22**, 337 (1993).
- [8] I. I. Rabi, *Phys. Rev.* **51**, 652 (1937).
- [9] L. Waldmann, *Z. Naturforsch. Teil. A* **12**, 660 (1957).
- [10] R.F. Snider, *J. Chem. Phys.* **32**, 1051 (1960).
- [11] B.C. Sanctuary and R.F. Snider, *J. Chem. Phys.* **55**, 1555 (1971).
- [12] R.E. Turner, *Phys. Rev. A* **28**, 3300 (1983); R.E. Turner and M. Senba, *ibid.* **29**, 2541 (1984); *J. Chem. Phys.* **84**, 3776 (1986).
- [13] R.E. Turner, R.F. Snider, and D.G. Fleming, *Phys. Rev. A* **41**, 1505 (1990).
- [14] F.M. Chen and R.F. Snider, *J. Chem. Phys.* **46**, 3937 (1967); **48**, 3185 (1968); **50**, 4082 (1969).
- [15] F.M. Chen, H. Moraal, and R.F. Snider, *J. Chem. Phys.* **57**, 542 (1972).
- [16] B.C. Sanctuary and R.F. Snider, *Can. J. Phys.* **53**, 707 (1975); **53**, 723 (1975); **53**, 739 (1975).
- [17] R.J. Duchovic, A.F. Wagner, R.E. Turner, D.M. Garner, and D.G. Fleming, *J. Chem. Phys.* **94**, 2794 (1991).
- [18] A.R. Edmonds, *Angular Momentum in Quantum Mechanics* (Princeton University Press, Princeton, 1960).
- [19] J.A.R. Coope, R.F. Snider, and F.R.W. McCourt, *J. Chem. Phys.* **43**, 2269 (1965).
- [20] J.A.R. Coope and R.F. Snider, *J. Math. Phys.* **11**, 1003 (1970).

- [21] J.A.R. Coope, *J. Math. Phys.* **11**, 1591 (1970).
- [22] P.W. Percival, J.C. Brodovitch, S.K. Leung, D. Yu, R.F. Kiefl, D.M. Garner, D.J. Arsenau, D.G. Fleming, A. Gonzales, J.R. Kempton, M. Senba, K. Venkateswaran, and S.F.J. Cox, *Chem. Phys. Lett.* **163**, 241 (1989).
- [23] F. James and M. Roos, MINUIT, Cern Computer 7600 Programme Library (1971).
- [24] W.H. Press, B.P. Flannery, S.A. Teukolsky, and W.T. Vetterling, *Numerical Recipes* (Cambridge University Press, Cambridge, 1990).